

235/2004

Raport Badawczy

RB/61/2004

Research Report

**Comparison of Numeral Methods for
Solution of Wheel – Rail
Contact Problems with Friction**

**A.Chudzikiewicz, A.Myśliński,
Z.Nagórski, J.Piotrkowski**

**Instytut Badań Systemowych
Polska Akademia Nauk**

**Systems Research Institute
Polish Academy of Sciences**



POLSKA AKADEMIA NAUK

Instytut Badań Systemowych

ul. Newelska 6

01-447 Warszawa

tel.: (+48) (22) 8373578

fax: (+48) (22) 8372772

Kierownik Pracowni zgłaszający pracę:
Prof. dr hab. inż. Kazimierz Malanowski

Warszawa 2004

Comparison of Numerical Methods for Solution of Thermoelastic Wheel - Rail Contact Problems with Friction

Andrzej Chudzikiewicz¹ and Andrzej Myśliński²

¹ Institute of Transport
Warsaw University of Technology
ul. Koszykowa 75
00-662 Warszawa, Poland

² System Research Institute
Polish Academy of Sciences
ul. Newelska 6
01 - 447 Warsaw, Poland

Zdzisław Nagórski³ and Jerzy Piotrowski³

³ Institute of Vehicels
Warsaw University of Technology
ul. Narbutta 84
02-524 Warszawa, Poland

1 Abstract

This paper deals with the numerical solution of wheel - rail rolling contact problems. The unilateral contact problem between a elastic body and a rigid foundation is considered. The contact with Coulomb friction law occurs at a portion of the boundary of the body. The contact condition is described in displacements. The friction coefficient is assumed to be bounded and suitable small. A frictional heat generation and heat transfer across the contact surface is assumed. The equilibrium state of this contact problem is described by the coupled hyperbolic variational inequality of the second order and a parabolic equation. This problem is solved

numerically using a quasistatic approach. The proposed method is compared with Green function approach and the method implemented in Fastsim algorithm. Numerical examples are provided and discussed.

Keywords: rolling contact, heat flow, numerical method

2 Introduction

The paper is concerned with the numerical solution of a contact problem for an elastic body. The contact with Coulomb friction occurs at a portion of the boundary of the body. The non-penetration condition governing the contact phenomenon is formulated in displacements. The friction coefficient is assumed to be bounded. The equilibrium state of this contact problem is described by the coupled system consisting of the hyperbolic variational inequality of the second order governing the displacement field and the parabolic equation governing the heat transfer.

The elastic rolling contact problem was considered by many authors (see literature in [8, 13]). The existence of solutions to the elastic static contact problem was shown in [8]. The non-penetration condition in [8] was formulated in displacements. One of the first rolling contact problem model was described in [16] where the Hertz model is used assuming that the contact zone and the normal contact stress are known. This model was developed and employed to calculate numerical solution of the wheel - rail wear problem in [16]. Since the contact phenomenon with friction is associated with the movement of bodies the dynamic contact

problems has been formulated.

The dynamic contact problems for the elastic bodies with nonpenetration condition formulated in displacement and the given friction have no solutions. Therefore to reflect the dynamic nature of the contact phenomenon either the quasistatic elastic contact problems have been considered or the contact problems for viscoelastic bodies with the nonpenetration condition formulated in velocities has been considered. The existence results and numerical methods for solving quasistatic elastic contact problems are provided in [13].

The effects of heat generation and heat transfer involving contact has been analysed in literature for many years (see [18]). Finite element formulations including thermomechanical coupling for contact problems has been presented in (see [1, 2, 4, 13]).

In [18] the Green function approach has been used used to solve the thermoelastic contact problems numerically. Papers where wear is included in the rolling contact model are less numerous. Reviewing paper [6] contains bibliography of papers dealing with contact and wear. In [16] Hertz contact model with Archard law of wear were employed to solve numerically wheel - rail contact problem. Models of contact with friction, heat generation and wear are introduced and discussed in [17].

In our previous paper, following [6] we used a quasistatic approach to solve this contact problem. This approach is based on assumption that for the observer moving with the rolling wheel the displacement of the rail is independent of time. Moreover we shall assume that the length of the rail is much bigger than the diameter of the wheel. We shall confine ourselves to the

case of small velocities of the wheel, i.e. we do not consider the vibration of the wheel. Under this assumption the rolling contact problem is described by an elliptic variational inequality instead of hyperbolic variational inequality. The thermal field is described by the parabolic equation.

The occurrence of sliding between wheel and rail results in the frictional heating of both bodies. High contact temperatures have to be taken into account to consider microstructural alternations as well as the decreasing the creep force curves. The first approach to calculate the contact temperature was based on the theory of heat conduction with moving heat sources (see papers of Blok and Jaeger). Tanvir provided an approximate solution of the rolling contact. Knothe et al., in a series of papers, presented a numerical method for solving rolling contact problem for arbitrarily distributed heat sources. All these works are confined to smooth surfaces and are based on the theory of Hertz for the mechanical contact problem.

The relation among wear, friction, fatigue and heat flow is also investigated in [19]. The wear, measured by the volume of the material removed, is a function of the entropy. Based on the Second and the Third Law of Thermodynamics, the wear is characterized as proportional to absolute temperature and entropy function and inverse proportional to a friction coefficient and a hardness pressure. The proposed law generalize the Archard's or Holm's wear law. The normalized wear coefficient has been determined experimentally.

In [13] the process of the dissipation of energy during sliding contact is investigated. Obtained experimental results indicate, that dissipated energy strongly depends on thermal properties of

the contacting bodies. On the other hand external loading and sliding velocity have almost no influence on energy dissipation. The wear appearance is an internal mechanism of the energy dissipation.

Temperature changes and phase transitions in sliding wheel - rail contact are calculated in [1] using the finite element method. Phase transitions occur due to frictional heat generation. Obtained results indicate that the phase is uniformly distributed in the wheel. The influence of the rail roughness on the wear of the wheel is investigated in [9]. Plastic zone occurs near the rail surface. This plastic zone depends on the friction coefficient as well as the creepage.

2.1 The goal of the present research

This paper extends results presented in [2, 3, 4, 5, 6]. After brief introduction of the thermoelastic model of the rolling contact problem in the framework of two-dimensional linear elasticity theory [2] the general coupled parabolic - hyperbolic system describing this physical problem is formulated. To solve numerically the discretized system we will decouple it into mechanical and thermal parts (see [2]). First, for a given temperature field we solve the mechanical part. In order to solve the mechanical part of this system we introduce a regularization of the friction conditions. Moreover, we replace the solving the hyperbolic inequality by solving an auxiliary optimization problem to calculate the displacement and stress fields in the whole domain. Newton method is employed to calculate tangent contact stress from regularized friction conditions. In the second step for the calculated displacement field we solve the thermal part of the system using the Newton method. The applications are for wheel - rail

systems. The numerical results are discussed. The obtained results are compared with results obtained using Green function approach and modified Fastsim algorithm.

3 Rolling Contact Problem

Consider deformations of an elastic strip lying on a rigid foundation (see Fig. 1). The strip has constant height h and occupies domain $\Omega \in R^2$ with the boundary Γ . A wheel rolls along the upper surface Γ_C of the strip. The wheel has radius r_0 , rotating speed ω and linear velocity V . The axis of the wheel is moving along a straight line at a constant altitude h_0 where $h_0 < h + r_0$, i.e., the wheel is pressed in the viscoelastic strip. It is assumed, that the head and tail ends of the strip are clamped, i.e., we assume that the length of the strip is much bigger than the radius of the wheel. Moreover it is assumed, that there is no mass forces in the strip. The body is clamped along a portion Γ_0 of the boundary Γ of the domain Ω . The contact conditions are prescribed on a portion Γ_C of the boundary Γ . Moreover, $\Gamma_0 \cap \Gamma_C = \emptyset$, $\Gamma = \Gamma_0 \cup \Gamma_C$. We denote by $u = (u_1, u_2)$, $u = u(x, t)$, $x \in \Omega$, $t \in [0, T]$, $T > 0$ a displacement of the strip and by $\theta = \theta(x, t)$ the absolute temperature of the strip.

In an equilibrium state the displacement u and the temperature θ of the strip satisfy the system

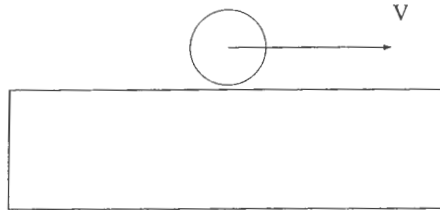


Figure 1: The wheel rolling over the strip.

of equations [1, 2, 7, 8, 17, 25]:

$$\rho \frac{\partial^2 \mathbf{u}}{\partial t^2} = A^* D A \mathbf{u} - \alpha(3\lambda + 2\gamma) \nabla \theta \quad \text{in } \Omega \times (0, T), \quad (1)$$

$$\rho c_p \frac{\partial \theta}{\partial t} = \bar{\kappa} \Delta \theta \quad \text{in } \Omega \times (0, T), \quad (2)$$

with initial and boundary conditions:

$$\mathbf{u} = 0 \quad \text{on } \Gamma_0 \times (0, T), \quad (3)$$

$$B^* D A \mathbf{u} = \mathbf{F} \quad \text{on } \Gamma_C \times (0, T), \quad (4)$$

$$\mathbf{u}(0) = \bar{\mathbf{u}}_0 \quad \mathbf{u}'(0) = \bar{\mathbf{u}}_1 \quad \text{in } \Omega, \quad (5)$$

$$\theta(0) = \bar{\theta} \quad \text{in } \Omega, \quad (6)$$

$$\frac{\partial \theta}{\partial n}(x, t) = q(t) \quad \text{on } \Gamma, \quad (7)$$

where $\mathbf{u}(0) = \mathbf{u}(x, 0)$, $\mathbf{u}' = d\mathbf{u}/dt$, $\bar{\mathbf{u}}_0, \bar{\mathbf{u}}_1, \bar{\theta}, q(t)$ are given functions, ρ is a mass density of the strip material, α is a coefficient of thermal expansion, $\bar{\kappa}$ is a thermal conductivity coefficient, c_p is a heat capacity coefficient, $\Gamma_0 = \Gamma \setminus \Gamma_C$, the operators A, B and D are defined as follows

[5]

$$A = \begin{bmatrix} \frac{\partial}{\partial x_1} & 0 \\ 0 & \frac{\partial}{\partial x_2} \\ \frac{\partial}{\partial x_2} & \frac{\partial}{\partial x_1} \end{bmatrix}, \quad B = \begin{bmatrix} n_1 & 0 \\ 0 & n_2 \\ n_2 & n_1 \end{bmatrix}, \quad D = \begin{bmatrix} \lambda + 2\gamma & \lambda & 0 \\ \lambda & \lambda + 2\gamma & 0 \\ 0 & 0 & \gamma \end{bmatrix} \quad (8)$$

where $\mathbf{n} = (n_1, n_2)$ is outward normal versor to the boundary Γ of the domain Ω , λ and γ are Lamé coefficients [8, 13], A^* denotes a transpose of A . By $\sigma = (\sigma_{11}, \sigma_{22}, \sigma_{12})$ and \mathbf{F} we denote the stress tensor in domain Ω and surface traction vector on the boundary Γ respectively. The surface traction vector $\mathbf{F} = (F_1, F_2)$ on the boundary Γ_C is a priori unknown and is given by

conditions of contact and friction. Under the assumptions that the strip displacement is small the contact conditions take a form [8, 17]:

$$u_2 + g_r + \leq 0, \quad F_2 \leq 0, \quad (u_2 + g_r)F_2 = 0 \quad \text{on } \Gamma_C \times (0, T), \quad (9)$$

$$g_r = r - r_0,$$

$$|F_1| \leq \mu |F_2|, \quad F_1 \frac{du_1}{dt} \leq 0, \quad (|F_1| - \mu |F_2|) \frac{du_1}{dt} = 0 \quad \text{on } \Gamma_C \times (0, T), \quad (10)$$

where μ is a friction coefficient and r is the distance between the center of the wheel and a point $x \in \Gamma_C$ lying on the boundary Γ_C of the strip Ω . Under suitable assumptions $g_r = h - h_0 + \sqrt{r_0^2 - (u_1 + x_1)^2}$. Conditions (9) - (10) describe the contact conditions. (9) is the nonpenetration condition. The wheel either has partly a common boundary with the rail, i.e. there is no normal displacement and appears nonzero reaction force or has no such boundary and the reaction force is equal to zero. (10) is Coulomb law of friction. If tangential force F_1 is less than the friction force μF_2 the wheel rolls without sliding. If the tangential force is equal to the friction force the sliding of the wheel over the rail occurs.

The original dynamic contact problem (1) - (10) is formulated in displacements. It is well known that, in general, this problem has no solutions. Therefore there are difficulties to solve it numerically. There are two approaches to deal with this difficulty. Taking into account the special features of this problem one can formulate it in the framework of the quasistatic approach. The second approach is based on adding the viscosity term and formulation of nonpenetration condition in velocities. In this paper we confine to the first approach only. The second approach is considered in [7].

4 Quasistatic Formulation

Let us recall from [4, 7] the the quasistatic formulation of the contact problem (1) - (6). Let be given an observer moving with the wheel with the constant linear velocity V . We shall assume:

- (i) the length of the strip is much bigger than the radius of the wheel,
- (ii) for the observer moving with a wheel the displacement of the strip does not depend on time,
- (iii) the velocity of the wheel is small enough, i.e. vibrations of wheel can not appear.

If the running velocity is constant the temperature very soon approach steady-state values.

We assume in the contact area the heat is generated due to friction and the heat flow rate is transformed completely into heat.

Let us introduce the new cartesian coordinate system $O'x'_1x'_2$ hooked in the middle of the wheel. The systems $O'x'_1x'_2$ and Ox_1x_2 are related by:

$$\begin{aligned}x'_1 &= x_1 - Vt, \\x'_2 &= x_2.\end{aligned}\tag{11}$$

Since by assumptions (i)-(iii) $u(x'_1, x'_2)$ does not depend on time we obtain:

$$\frac{du}{dt}(x'_1, x'_2) = \frac{du}{dt}(x_1 - Vt, x_2, t) = 0.\tag{12}$$

It implies

$$\frac{du}{dt} = -V \frac{du}{dx_1} \quad \text{and} \quad \frac{d^2u}{dt^2} = V^2 \frac{d^2u}{dx_1^2}.\tag{13}$$

Using the same argument we obtain:

$$\frac{d\theta}{dt} = -V \frac{d\theta}{dx_1}, \quad \frac{dw}{dt} = -V \frac{dw}{dx_1}. \quad (14)$$

Let Ω denotes now the moving part of the strip seen by the observer. Taking into account (11) quasistatic approximation of the problem (1) – (3) takes the form:

Find u and θ satisfying

$$A^*DAu - \rho V^2 u_{11} - \alpha(3\lambda + 2\gamma)\nabla\theta = 0 \quad \text{in } \Omega, \quad (15)$$

$$-V \frac{\partial\theta}{\partial x_1} = \kappa \frac{\partial^2\theta}{\partial x_2^2} \quad \text{in } \Omega, \quad (16)$$

$$u = 0 \quad \text{on } \Gamma_0, \quad (17)$$

$$B^*DAu = F \quad \text{on } \Gamma_C, \quad (18)$$

$$u_2 + g_r + w \leq 0, \quad F_2 \leq 0, \quad (u_2 + g_r + w)F_2 = 0 \quad \text{on } \Gamma_C$$

$$|F_1| \leq \mu |F_2|, \quad F_1 u_{1,1} \leq 0, \quad (|F_1| - \mu |F_2|)u_{1,1} = 0 \quad \text{on } \Gamma_C, \quad (19)$$

$$-\bar{\kappa} \frac{\partial\theta}{\partial x_2} = \bar{\alpha} \left[\frac{\theta}{r} F_2(x) + \left(1 - \frac{k\rho c_p \theta}{\mu}\right) \mu V F_2(x) \right] \quad \text{on } \Gamma_C, \quad (20)$$

where $u_{i,j} = \frac{\partial u_i}{\partial x_j}$, $u_{i,jk} = \frac{\partial^2 u_i}{\partial x_j \partial x_k}$, $i, j, k = 1, 2$, $u_{ij} = (u_{m,ij})_{m=1,2}$, $i, j = 1, 2$, $\kappa = \bar{\kappa}/\rho c_p$ is the thermal diffusivity coefficient, $\bar{\alpha}$ represents the fraction of frictional heat flow rate entering the rail, r is thermal resistance constant. There are also given initial conditions (5) - (6). We assume in (19) the heat flows through the contact surface only, therefore $\theta = 0$ on Γ_0 .

4.1 Numerical Realization

Problem (15) - (20) is a coupled thermoviscoelastic problem since the contact traction will depend on the thermal distortion of the bodies. On the other hand, the amount of heat generated due to friction will depend on the contact traction. The main solution strategies for coupled problems are global solution algorithms where the differential systems for the different variables are solved together or operator splitting methods. In this paper we employ operator split algorithm.

The conceptual algorithm for solving (15) - (20) is as follows [2]:

Step 1 : Choose $\theta = \theta^0$. Choose $\eta \in (0, 1)$. Set $k = 0$.

Step 2 : For given θ^k find u^k and σ_N^k satisfying system

(15) and boundary conditions (17) - (19).

Step 3 : For given u^k and σ_N^k find θ^{k+1} satisfying

equations (16) and (20) respectively.

Step 4 : If $\|\theta^{k+1} - \theta^k\| \leq \eta$, Stop. Otherwise : set $k = k + 1$, go to Step 2.

For the convergence of the operator split algorithm using Fixed Point Theorem see literature in [2]. Let us present in details the algorithms for solving discrete mechanical and thermal subproblems.

4.2 Numerical Results

Problem (15)-(20) was solved numerically using the described in the previous section algorithms. Polygonal domain Ω given by

$$\Omega = \{(x_1, x_2) \in R^2 : x_1 \in (-2, 2), x_2 \in (0, 1)\} \quad (21)$$

was divided into 192 triangles. The contact boundary Γ_C is modeled by 13 nodes. The Lamé constants were $\lambda = 11.66 \cdot 10^{10}$ [N/m²], $\gamma = 8.2 \cdot 10^{10}$ [N/m²], the density $\rho = 7.8 \cdot 10^3$ [kg/m³], the velocity $V = 10$ [m/s], radius of the wheel $r = 0.46$ [m]. The penetration of the wheel was taken as $\delta = 0.1 \cdot 10^{-3}$ [m]. The heat capacity $c = 460$ J/kgK, thermal diffusivity coefficient $\kappa = 1,4410^{-5}$ m²/s, thermal expansion coefficient $\gamma = 1210^{-6}$. The friction coefficient $\mu = 0.4$, the thermal resistance coefficient $r = 1000$ KNs/J. \bar{u}_0 and \bar{u}_1 in (5) as well as $\bar{\theta}$ in (6) are equal to 0. The results are showed on Fig. 2 and Fig. 3.

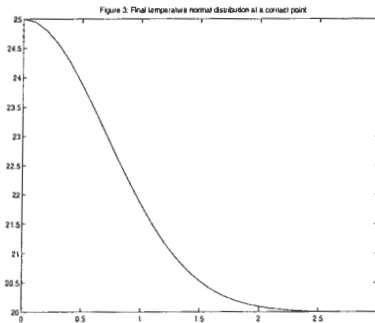


Figure 2: Temperature normal distribution at a contact point.

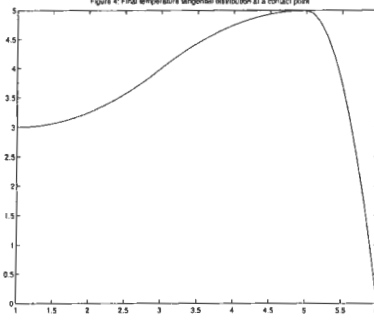


Figure 3: Temperature tangential distribution at a contact point.

5 Green Function Approach

Similar problem was solved in [16] where the solutions to system (15) - (20) were calculated analytically using Green functions.

In [10], assuming the static wheel load, the area of contact and the pressure distribution may be calculated with the Hertz's theory. The area of contact is assumed to be elliptical and the normal pressure distribution is given by

$$p(x, y) = p_0 \sqrt{1 - \frac{x^2}{a^2} - \frac{y^2}{b^2}}, \quad (22)$$

with the maximal pressure p_0

$$p_0 = \frac{3N}{2\pi ab}, \quad (23)$$

for the normal load N and the semi - axes a in rolling direction and b of contact ellipse.

The existence of the tangential force T transmitted between the wheel and the rail implies the occurrence of a mean relative velocity in the contact point. High contact temperatures are to be expected only with the transmission of tractive or braking forces at high relative velocities,

In this case sliding is assumed to occur within the whole contact area and the tangential force

$T = \mu N$, μ denotes a constant friction coefficient.

From the point of view of an observer fixed to the wheel, the contact patch moves with respect to the wheel surface and the frictional heating within the contact patch is a time - dependent heat source. The thermal penetration depth, during the contact of wheel and rail, is equal to

$$\delta = \frac{a}{\sqrt{L}} \quad (24)$$

and is very small compared to the size of the contact patch. It depends on the non - dimensional Péclet number

$$L = \frac{av}{2\kappa} \quad (25)$$

where a is the length of the contact semi axis, v denotes the speed of the moving heat source and the thermal diffusivity

$$\kappa = \frac{\lambda}{\rho c} \quad (26)$$

combining the material properties λ (thermal conductivity), ρ (mass density) and c (specific heat). Note, that L may be interpreted as the ratio of the surface speed to the rate of the diffusion of the heat into the solid. If $L > 10$ heat conduction appears only perpendicular to the contact plane, i.e., in z - direction. In wheel - rail systems typical value is $L = 5300$.

5.0.1 Analytical Solution

The heat flow in z direction is governed by:

$$\kappa \frac{\partial^2 \theta}{\partial z^2} = \frac{\partial \theta}{\partial t}, \quad (27)$$

with the initial condition

$$\theta(z, 0) = 0, \quad (28)$$

and the boundary condition

$$-\lambda \frac{\partial \theta}{\partial z}(0, t) = \dot{q}(t), \quad (29)$$

The solution to (27) - 29) is given by

$$\theta(z, t) = \frac{1}{\beta \sqrt{\pi}} \int_0^t \dot{q}(t - t') \exp\left\{-\frac{z^2}{4\kappa t'}\right\} \frac{dt'}{\sqrt{t'}}, \quad (30)$$

with the thermal penetration coefficient

$$\beta = \frac{\lambda}{\sqrt{\kappa}}. \quad (31)$$

Let us introduce the dimensionless coordinates

$$\xi = \frac{x}{a}, \quad \zeta = \frac{z}{\delta}.$$

The temperature of the wheel is equal to

$$\theta_w(\xi, \zeta) = \frac{1}{\beta_w} \sqrt{\frac{a}{\pi v_w}} \int_{-1}^{\xi} \dot{q}_w(\xi') \exp\left(-\frac{\zeta^2}{2(\xi - \xi')}\right) \frac{d\xi'}{\sqrt{\xi - \xi'}}, \quad (32)$$

for the wheel with $v_w = v_0 + v_s$ and

$$\theta_r(\xi, \zeta) = \frac{1}{\beta_r} \sqrt{\frac{a}{\pi v_r}} \int_{-1}^{\xi} \dot{q}_r(\xi') \exp\left(-\frac{\zeta^2}{2(\xi - \xi')}\right) \frac{d\xi'}{\sqrt{\xi - \xi'}}, \quad (33)$$

for the rail with $v_r = v_0$. The analytical solution (32) is simple to calculate if we assume a constant heat flow rate \dot{q}_w at the wheel surface within the contact path. For $-1 \leq \xi \leq 1$, we get

$$\theta_w(\xi, \zeta) = \frac{\dot{q}_w}{\beta_w} \sqrt{\frac{2a}{v_w}} \left\{ \sqrt{\frac{2(\xi + 1)}{\pi}} \exp\left(-\frac{\zeta^2}{2(\xi + 1)}\right) - \zeta \operatorname{erfc}\left(\frac{\zeta}{\sqrt{2(\xi + 1)}}\right) \right\}, \quad (34)$$

where the complement of the error function is equal to

$$\operatorname{erfc}(s) = 1 - \operatorname{erf}(s) = 1 - \frac{2}{\sqrt{\pi}} \int_0^s e^{-\omega^2} d\omega. \quad (35)$$

Outside the contact area there is now frictional heating. Neglecting convection, the heat flow rate is zero and the analytical solution for $\xi > 1$ is equal to

$$\begin{aligned} \theta_w(\xi, \zeta) = \frac{\dot{q}_w}{\beta_w} \sqrt{\frac{2a}{v_w}} \{ & [\sqrt{\frac{2(\xi+1)}{\pi}} \exp(-\frac{\zeta^2}{2(\xi+1)}) - \zeta \operatorname{erfc}(\frac{\zeta}{\sqrt{2(\xi+1)}})] \\ & - [\sqrt{\frac{2(\xi-1)}{\pi}} \exp(-\frac{\zeta^2}{2(\xi-1)}) - \zeta \operatorname{erfc}(\frac{\zeta}{\sqrt{2(\xi-1)}})] \}. \end{aligned} \quad (36)$$

5.0.2 Analytical solution for constant heat flow rate

Assuming the constant values of the coefficient of friction μ and the sliding velocity v_s the frictional power dissipation rate in the contact patch is equal to:

$$\dot{q}(\xi) = \mu v_s p_0 \sqrt{1 - \xi^2}, \quad \xi = 1 - \frac{x^2}{a^2}. \quad (37)$$

The all frictional power dissipation is transformed into heat flowing into the material of wheel and rail. Therefore

$$\dot{q} = \varepsilon \dot{q}_w + (1 - \varepsilon) \dot{q}_r, \quad (38)$$

where ε is a heat partitioning factor. The maximum temperature of wheel has been calculated as:

$$\theta_{max} = 1.253 \frac{\varepsilon \mu v_s p_0}{\beta_w} \sqrt{\frac{a}{v_w}}. \quad (39)$$

This maximum temperature occurs at the trailing edge of the contact patch.

The temperature of wheel is also dependent on the heat flow from the hot wheel into the cold rail due to conduction through the contact patch as well as into ambient air by the convection at the free surfaces.

5.1 Conduction

Consider now the heat conduction from wheel into rail. The continuous frictional heating on the wheel surface results in wheel temperature increase in time. When a point on the wheel surface comes into the contact area again the temperatures of wheel and rail are different. Since after the one revolution of the wheel the temperature gradient is small the next contact of a point on the surface of the wheel and the rail can be treated as the contact between the two semi - infinite bodies with different initial temperatures coming into contact at time $t=0$. Assuming that the initial temperatures of wheel and rail are:

$$\theta_w(z, t = 0) = \theta_{w0}, \quad \theta_r(z, t = 0) = 0, \quad (40)$$

it can be shown the surface temperature attains a constant value θ_m equal to:

$$\theta_m = \varepsilon \theta_{w0}. \quad (41)$$

The heat flow rate through the contact patch from the hot wheel into the cold rail is then

$$\dot{q}_w(\chi) = \varepsilon \beta_r \theta_{w0} \sqrt{\frac{v_0}{\pi a(\chi + 1)}} = -\dot{q}_r(\chi). \quad (42)$$

This heat flow rate implies the following total heat flow per unit width

$$Q_{\text{rail}}/b^* = a \int_{-1}^1 \dot{q}_w(\chi) d\chi = -\varepsilon \beta_r \theta_{w0} \sqrt{\frac{8av_0}{\pi}}. \quad (43)$$

Since outside the contact zone there is no heat flow from the wheel into the rail, the surface temperature of the wheel is equal to

$$\theta_w(\chi, \zeta = 0) = \theta_{w0} \left\{ 1 - \frac{2}{\pi} (1 - \varepsilon) \arcsin \sqrt{\frac{2}{\chi + 1}} \right\}, \text{ for } |\chi| > 1. \quad (44)$$

5.2 Heat Convection

Consider a heat flow due to convection outside the contact zone. The heat flows from the wheel into ambient air by convection at the free surfaces. This convection phenomenon is forced by the rotation of the wheel. The boundary condition outside the contact area has the form:

$$\lambda_w \frac{\partial \theta_w}{\partial z}(x, z = 0) = \alpha \theta_w(x, z = 0), \quad (45)$$

where $x > a$ and α is the heat transfer coefficient. This coefficient is calculated using empirical formula. Typical values of α are in the range of $10 - 100 \text{ W/Km}^2$.

Another measure of the convection from a solid into a fluid is the Biot number

$$Bi = \frac{\alpha d}{\lambda_w}, \quad (46)$$

where d is the main characteristic length (here equal to $2a$). For small Biot numbers, i.e., $Bi < 0, 1$ the temperature gradient in the solid can be neglected for the calculation of the convective heat transfer. Assuming that the average wheel temperature is constant at θ_{w0} we obtain the heat flow rate as equal to

$$\dot{q}_{convection} = -\alpha \theta_w, \quad (47)$$

at the surface and the total heat flow per unit width is

$$\dot{Q}_{convection}/b^* = -2\pi r_0 \alpha \theta_{w0} \quad (48)$$

Comparing

$$\frac{\dot{Q}_{convection}}{\dot{Q}_{rail}} = \frac{\alpha T_0}{\varepsilon \beta_r} \sqrt{\frac{\pi^3}{2a v_0}} \quad (49)$$

we obtain this ratio is less than 1%. Numerical experiments indicate that the convective heat transfer can be neglected except for very big, unrealistic, values of the heat transfer coefficient.

5.3 Steady - state wheel temperature

The heat loss due to conduction into the rail is proportional to the initial surface temperature of the wheel. This loss is equal to the frictional heating at a value of the initial temperature calculated from the energy balance

$$\frac{\varepsilon P_{friction}}{b^*} + \frac{\dot{Q}_{rail}}{b^*} = 0 \quad (50)$$

where $\varepsilon P_{friction}$ is a fraction of the frictional power dissipation

$$P_{friction} = \mu v_s N = \frac{\pi}{2} \mu p_0 a b^* v_s \quad (51)$$

flowing into the wheel. From (42) it follows that steady - state wheel temperature equals to

$$\theta_{\infty} = \frac{\mu v_s p_0}{\beta_r} \sqrt{\frac{\pi^3 a}{32 v_0}} \quad (52)$$

The value of this temperature depends on the thermal penetration coefficient of the rail only.

Numerical experiments indicate that the surface temperature comes near a steady - state after

30 - 120 min, depending on the operating conditions. Assuming the constant heat flow rate,

we have

$$\frac{\theta_{\infty}}{\theta_{mean}} = \frac{1}{0.836(1 - \varepsilon)} \sqrt{\frac{\pi^3}{32}} \quad (53)$$

The average contact temperature results from the current frictional heating and from the average wheel temperature in steady - state, i.e.,

$$\theta_{mean,\infty} = \theta_{mean} + \varepsilon\theta_{\infty}, \quad (54)$$

For $\varepsilon = 0.5$ the average contact temperature $\theta_{mean,\infty}$ in steady - state is twice as high as the average contact temperature θ_{mean} for the first contact of the cold wheel. It means, that the body in continuous contact is an insulator. Thus all the frictional heating flows into the rail and doubles the contact temperature.

The temperature field in the wheel, calculated with the initial value θ_{∞} , remains constant at this value. The average bulk temperature of the wheel does not change due to lack of the resulting heat flow. The oscillating surface temperature is due to the different distributions of the heat flow rates resulting from frictional heating and rail contact. Outside the contact zone, the gradient of temperature in perpendicular direction is disappearing and the temperature in the wheel will be constant again.

5.4 Numerical Results

Table 1. Summary of results for elliptical contact area (all temperatures in °C).

	Low speed	High speed
Instantaneous contact temperature		
Maximal Temperature	149,7	86,4
Average contact temperature	81,7	47,1
Steady - state temperature without convection	182,6	105,4
	173,7	100,3
$\alpha = 10W/Km^2$	153,5	95,0
	159,0	95,1
$\alpha = 30W/Km^2$	116,4	79,4
	140,3	87,2
$\alpha = 100W/Km^2$	63	50,3
	113,4	72,5
$\alpha = 1000W/Km^2$	9,1	8,8
	86,3	51,6

Table 1 gives results of computations for two different vehicle speeds. Low speed means vehicle speed equal to 30 m/s, while high speed 90 m/s. Longitudinal sliding velocity is equal to 1 m/s for low speed case and 3 m/s for high speed case. In both cases normal load is equal to 100 kN, and frictional power dissipation is equal to 30 Kw. Coefficient of friction is equal to 0,3 for low speed case and 0,1 for high speed case.

The results show that the temperature decreases with increasing vehicle speed. The steady state temperature depends mainly on heat conduction from wheel into rail. It is even lower if convection is also taken into account. If the heat transfer coefficient α is in the range of 50 - 100 W/Km^2 , the heat flow into an ambient air is nearly equal to the heat conduction from from wheel into air. Thus θ_{∞} is only half as high as without convection. For α overestimated, the average wheel temperature would be nearly equal to ambient temperature.

Obtained maximum contact temperatures are not high enough to explain thermally induced phase transformations. This may only be the case with extreme conditions, i.e. blocking wheels where the sliding velocity is equal to the vehicle speed. On the other hand contact

temperatures increase thermal stresses. It has been shown, thermal stresses in railway wheels and rails can be in the same order of magnitude as the mechanical stresses. This may cause plastic deformations, residual stresses, work hardening at the surfaces of wheel and rail. Since the thermal penetration depth is small, thermally induced plastic deformations are restricted to a very thin surface layer.

6 Modified Fastsim algorithm

The problem (1) - (10) has been also solved in [21, 22] using the modified Fastsim algorithm combined with the finite difference method. The Fastsim algorithm was used to calculate the frictional power density, i.e., a heat generated due to friction. The finite difference method was used to solve the heat governing equations. Let us describe details.

6.1 Calculation of Normal Force

The wheel is assumed to have conical rolling surfaces. There are two rails parallel to each other, so positioned vertically that rolling radii on conical surfaces may be different. Since the rolling radii on conical surfaces of the wheel are different, the longitudinal creepages occur during rolling. Due to conical rolling surfaces of the wheel the spin creepage appear in both contact zones. The normal and tangential forces in the contact zones depend on the wheel geometry, coefficients of friction as well as the vertical load Q of the wheel. The calculation of the normal force N is based on Kalker theory. The normal and tangential components of the forces loading the wheel satisfy the system of three, nonlinear algebraic equations. To make the equations explicit tangential forces T_{x_i} and T_{y_i} , $i = 1, 2$ by following linear functions of

creepages

$$T_{x_i} = E_{x_i} N_i \nu_{x_i}, \quad T_{y_i} = E_{y_i} N_i (\nu_{y_i} + c_i \Phi_i)$$

where E_{x_i} and E_{y_i} are coefficients, c_i is an equivalent radius of the contact zone. Longitudinal creepages ν_{x_i} , ν_{y_i} , and spin creepage Φ_i are defined by

$$\nu_{x_i} = \frac{r_2 - r_1}{2r} + (-1)^i \frac{r_i}{r} \hat{\theta}, \quad \nu_{y_i} = \frac{r_i}{r} \alpha \frac{1 + \tilde{\theta}}{\cos(\gamma_i)},$$

$$\Phi_i = \frac{1 + \tilde{\theta}}{r} \sin(\gamma_i),$$

r_i are wheel radii, $r = 0.5(r_1 + r_2)$, α denotes yaw angle, γ_i denote the angle between horizontal and tangential lines, $\tilde{\theta}$ is a small unknown number. Using the normalized creep forces f_{x_i} and f_{y_i} as well as frictions coefficients μ_i the tangential forces are equal to

$$T_{x_i} = \mu_i N_i f_{x_i}, \quad T_{y_i} = \mu_i N_i f_{y_i}$$

Comparing the above expressions for tangential forces the unknown coefficients can be determined. Assuming that the inertia of the wheel is neglected, and transforming the system of equilibrium equations, the normal force $N = \{N_i\}$ is calculated from the system

$$AN = Q, \tag{55}$$

where $A = \{a_{ij}\}_{i,j=1}^2$ denotes the matrix of coefficients dependent on E_{x_i} , E_{y_i} and creepages.

For a calculated normal force N , the number $\tilde{\theta}$ is calculated. Fixed point method is applied to solve the equation (55).

6.2 Calculation of Frictional Power Density

Since the Kalker table contains creep forces it can not be used for the calculation of frictional power density P_d . This density can be calculated using the modified Fastsim algorithm. Consider a wheel rolling in a time interval $[0, T]$, $T > 0$, given. A wheel is assumed to be a discretized Winkler foundation. The modified Fastsim algorithm calculating frictional power density P_d reads: having calculated the tangential traction at time t' , the tangential traction p_h at time $t > t'$ is calculated as

$$p_h = p' - \frac{t - t'}{L} w$$

Next the power density $P - D$ is calculated according to formulae

$$\begin{aligned} &\text{if } |p_h| \leq \mu p_z \text{ then } p = p_h \text{ and } P_d = 0, \quad s = 0, \\ &\text{else } p = \frac{p_h}{|p_h|} \mu p_z, \quad P_d = p \cdot w + V \left(\frac{3N\mu}{2\pi a^2 b} \right)^2 Lx, \quad s = -\frac{P_d}{p} \end{aligned}$$

where L is an elasticity parameter, μ is a coefficient of friction, V constant rolling velocity, and w denotes rigid slip corresponding the unit velocity of rolling equal to

$$w = [w_x, w_y], \quad w_x = V(\nu_x - y\Phi), \quad w_y = V(\nu_y + x\Phi)$$

Moreover

$$p' = p(t') \text{ tangential traction at the instant of time } t' < t$$

$$p = p(t) \text{ tangential traction at the instant of time } t,$$

Normal pressure p_z is equal to

$$p_z = \frac{3N}{2\pi ab} \sqrt{1 - \frac{x^2}{a^2} - \frac{y^2}{b^2}},$$

where N denotes a normal force and a, b are semi - axes of contact ellipse. s is a slip velocity equal to

$$s = w + u.$$

6.3 Calculation of Temperature

For the sake of simplicity, a rail is considered as a parallelepiped occupying domain

$$\Omega = [0 \ a] \times [0 \ b] \times [0 \ c],$$

where $a, b, c > 0$, are given constants. This parallelepiped is divided into the small cells having dimensions dx, dy and dz . The heat source is assumed to move over the contact area $C \subset R^2$ lying on the outer surface of the rail $z = 0$ with velocity V . The contact area C is assumed to be elliptical. By $\theta = \theta(x, y, z, t)$, $(x, y, z) \in \Omega, t \in [0, T]$, we denote a temperature of the wheel.

The transient heat conduction in the frame of three dimensional model of the rail is described by the Fourier partial differential equation, i.e.,

$$\frac{\partial \theta}{\partial t} = \alpha \Delta \theta \text{ in } \Omega \times (0, T), \quad (56)$$

where $\alpha = \frac{\lambda}{c_p \rho}$ denotes a temperature compensation coefficient, λ is a conductivity coefficient, c_p is a characteristic heat and ρ denotes a mass density. The following boundary conditions are prescribed

$$\frac{\partial \theta}{\partial y} = 0 \text{ on } y = 0, b, \quad (57)$$

$$\theta = 0 \text{ on } x = 0, x = a, x = b, z = c. \quad (58)$$

On the outer surface of the rail $z = 0$ the following boundary condition is assumed

$$\frac{\partial \theta}{\partial z} = P_d \text{ on } z = 0 \text{ and } (x, y) \in C, \quad (59)$$

$$\frac{\partial \theta}{\partial z} = \kappa(\theta - \theta_g) \text{ on } z = 0 \text{ and } (x, y) \notin C \quad (60)$$

$$(61)$$

Moreover the initial condition have the form

$$\theta(x, y, z, 0) = 0 \text{ in } x \in \Omega,$$

$$\frac{\partial \theta}{\partial n}(x, y, z, 0) = 0 \text{ on } z = 0.$$

The computations have been performed using the finite difference method with the explicit Euler discretization. The discrete rail model has been build in the Excel spreadsheet. Each cell of a spreadsheet is equivalent each cell of a rail. The dimensions of a cell are equal to $d = dx = dy = dz$. To calculate the value of temperature θ in time t in each cell, the values of temperatures in six adjacent cells in time $t - 1$ are used. The difference scheme stability condition has the form

$$V \geq \frac{6\alpha}{d}.$$

6.4 Numerical Results

The computations has been performed for $\rho = 7680 \text{ kg/m}^3$, $\lambda = 54 \text{ W/(mK)}$, $c_p = 460 \text{ J/(kgK)}$, $dx = dy = dz = 0,001 \text{ m}$. Contact heat source is assumed to move with the velocity $V = 1 \text{ m/s}$. Fig. 4 and Fig. 5 display the temperature distribution for the circular contact area and the constant density heat source q . For $q = 1 \text{ W/mm}^2$ the temperature increase is

5,5 K. For the density heat source $q = 10W/mm^2$ the temperature increase is 55 K. The temperature within the contact patch sharply increases. After the particle leave the contact zone, the temperature falls. The temperature also rapidly decreases inside the rail to 1,5K and 15,5K respectively.

Fig. 6 and Fig. 7 show the temperature distribution for the elliptic contact area and the constant density heat sources: $q = 1W/mm^2$ and $q = 10W/mm^2$. Although the maximal temperatures are similar in this case the thermal trace on the surface of the rail is much bigger than in the circular contact area.

[22] reports also the temperature distribution obtained for irregular density heat source with two maximal values $q_{max} = 2,4W/mm^2$ moving with velocity $V = 1m/s$. The reported maximal temperature increase in the contact zone is equal to 2,4 K. The thermal trace on the surface of the rail is much wider and much longer than in previous cases.

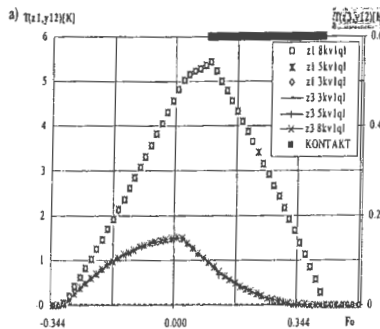


Figure 4: Temperature tangential distribution. Circular contact. $q = 1$.

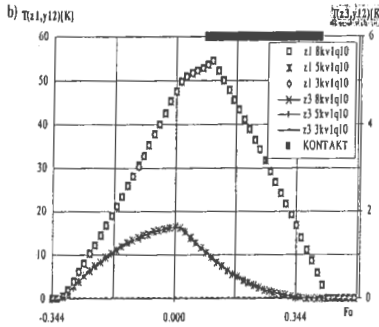


Figure 5: Temperature tangential distribution. Circular contact. $q = 10$.

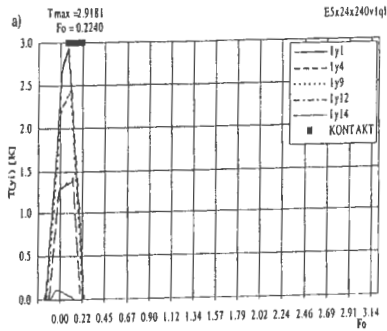


Figure 6: Temperature tangential distribution. Elliptic contact. $q = 1$.

7 Conclusions

The obtained results indicate that mechanical factors give rise to thermal effects which should be observable as the surface temperature field. The results obtained due to the quasistatic method and the FastSim method are very similar. The increase of the temperature and its distribution have the same character and magnitude. These results differ significantly from the results reported in [10], where much larger temperature increase is reported. Moreover as follows from Table 1, the higher the speed, the lower the temperature increase. The dependence

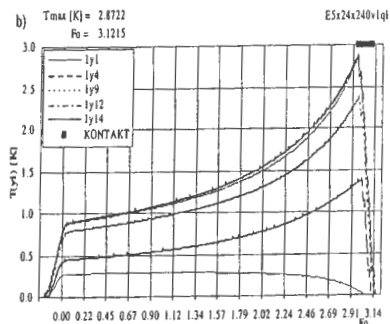


Figure 7: Temperature tangential distribution. Elliptic contact. $q = 1$. Final time.

of the contact temperature on sliding velocity and on the friction coefficient dependent on sliding velocity is subject of further research.

References

- [1] Ahlström, J., Karlsson, B., Modelling of heat conduction and phase transformation during sliding of railway wheels, *Wear*, Vol. 253, No. 1 -2, pp. 291 - 300, 2002.
- [2] Chudzikiewicz, A., Myśliński, A., Wheel - Rail Contact Problem with Wear and Heat Flow, *Proceedings of the 7 VSDIA Conference*, pp. 149 - 157, 2002.
- [3] Chudzikiewicz, A. - Kalker, J.J., Wheel - Rail wear calculations with Fastsim routine, *The Archives of Transport*, 1990, pp. 9-27, 1990.
- [4] Chudzikiewicz, A., Myśliński, A., On Thermoelastic Wheel - Rail Contact Problem with Wear, Preprint, Warsaw University of Technology, 2000.

- [5] Chudzikiewicz, A., Żochowski, A., Myslinski, A., Quasistatic versus Kalker approach for solving rolling contact problems, *The Archive of Transport*, pp. 103 – 120, 1992.
- [6] Chudzikiewicz, A., *Wear of Wheel/Rail Systems*, Preprint, Warsaw University of Technology, 1999.
- [7] Chudzikiewicz, A. and Myśliński, A., Augmented Lagrangian Approach for Wheel - Rail Thermoelastic Contact Problem with Friction and Wear. *Preprint*, Systems Research Institute, Warsaw, Poland, 2002.
- [8] Duvaut, G. and Lions, J.L., *Les inequations en mecanique et en physique*, Dunod, Paris, 1972.
- [9] Daves, W., Fisher, F.D.: Modelling of the plastification near the rough surface of a rail by the wheel - rail contact, *Wear*, Vol. 253, No 1 - 2, pp. 241 - 246, 2002.
- [10] Ertz, M., Knothe, K. : A comparison of Analytical and Numerical Methods for the calculation of temperatures in wheel/rail contact, *Wear*, Vol. 253, pp. 498 - 508, 2002.
- [11] Fisher, F.D., Werner, K., Knothe, K. : The Surface Temperature of a Halfplane Heated by Friction and Cooled by Convection, *Z. Angew. Math. Mech.*, , Vol. 81, pp. 75 - 81, 2001.
- [12] Gupta, V., Hahn, G.T., Bastias, P.C., Rubin, C.A., Thermal - Mechanical Modelling of the Rolling - plus - Sliding with Frictional Heating of a Locomotive Wheel, *J. Eng. Ind.*, Vol. 117, pp. 418 - 422, 1995.

- [13] Han, W. and Sofonea, M., *Quasistatic Contact Problems in Viscoelasticity and Viscoplasticity*. AMS/IP Studies in Advanced Mathematics, **30**, 442 pp, 2002.
- [14] Johansson, L., Numerical Simulation of Contact Pressure Evolution in Fretting, *Journal of Tribology*, pp. 247 – 254, 1994.
- [15] Jäger, J., New analytical solutions for a flat rounded punch compared with FEM, *Computational Methods in Contact Mechanics V*, Eds.: J. Dominguez, C.A. Brebia, Wessex Institute of Technology, WIT Press, Southampton, pp. 307 - 316, 2001.
- [16] Kalker, J.J., *Three dimensional elastic bodies in rolling contact*, Kluwer Academic Publishers, 1990.
- [17] Klabrung, A., Large Displacement Frictional Contact: A Continuum Framework for Finite Element Discretization, 1995. (p. 237 – 253).
- [18] Knothe, K., Liebelt, S., Determination of temperatures for sliding contact with applications for wheel-rail systems, *Wear*, pp. 91 – 99, 1995.
- [19] Ling, F.F, Bryant, K.L., Doelling, K.L.: On irreversible thermodynamics for wear prediction, *Wear*, Vol. 253, Issues 11 - 12, pp. 1165 - 1172.
- [20] Myśliński, A., Augmented Lagrangian Techniques for Shape Optimal Design of Dynamic Contact Problems, Proceedings of the Fourth World Congress of Structural and Multidisciplinary Optimization, CD ROM, 2001.

- [21] Nagórski, Z., Piotrowski, J., Szolc, T., Parametric Analysis of the Thermal Trace Caused by Medium Frequency Wheel - Rail Contact Excitation, *18 - th International Association of Vehicle System Dynamics Symposium*, Atsugi - Kanagawa, Japan, 24 - 30 August, 2003, pp. 288 - 290.
- [22] Nagórski, Z., Piotrowski, J., Numerical Simulation and Preliminary Experimental Tests on Thermal Effects in Rolling Contact, *XIV Polish - German Seminar "Development Trends in Design of Machines and Vehicles*, Warsaw University of Technology, Warsaw, June 10 - 11, 2002.
- [23] Telega, J., Variational Methods in Contact Problems of Mechanics(in Russian). *Advances in Mechanics*, pp. 3-95, 1987.
- [24] Tworzydło, W.W., Cecot, W., Oden, J.T., Yew, C.H., Computational micro and macroscopic models of contact and friction: formulation, approach and applications, *Wear*, Vol 220, pp. 113 - 140, 1998.
- [25] Strömberg, N., Johansson, L., Klåbring, A., Derivation and Analysis of a Generalized Standard Model for Contact, Friction and Wear, *International Journal of Solids and Structures*, pp. 1817 - 1836, 1996.

